Dimensional analysis of the earthquake-induced pounding between inelastic structures

Bulletin of Earthquake Engineering
Official Publication of the European Association for Earthquake Engineering

ISSN 1570-761X
Volume 9
Number 2

Bull Earthquake Eng (2011)
9:561-579
DOI 10.1007/
s10518-010-9220-8

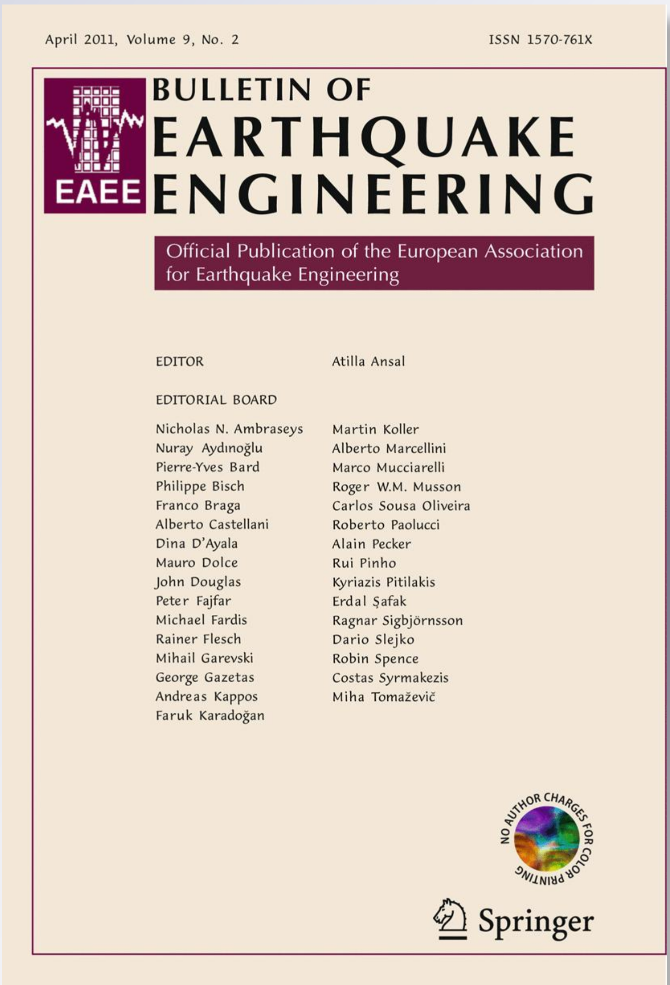

Springer

Bull Earthquake Eng (2011) 9:561–579
DOI 10.1007/s10518-010-9220-8

ORIGINAL RESEARCH PAPER

Dimensional analysis of the earthquake-induced pounding between inelastic structures

Elias G. Dimitrakopoulos · Nicos Makris · Andreas J. Kappos

Received: 18 January 2010 / Accepted: 19 October 2010 / Published online: 3 November 2010

Abstract In this paper the seismic response of inelastic structures with unilateral contact is revisited with dimensional analysis. All physically realizable contact types are captured via a non-smooth complementarity approach. The implementation of formal dimensional analysis leads to a condensed presentation of the response and unveils remarkable order even though two different types of non-linearity coexist in the response: the boundary non-linearity of unilateral contact and the inelastic behaviour of the structure itself. It is shown that regardless the intensity and frequency content of the excitation, all response spectra become self-similar when expressed in the appropriate dimensionless terms. The proposed approach hinges upon the notion of the energetic length scale of an excitation which measures the persistence of ground shaking to impose deformation demands. Using the concept of persistency which is defined for excitations with or without distinct pulses, the response is scaled via meaningful novel intensity measures: the dimensionless gap and the dimensionless yield displacement. The study confirms that contact may have a different effect on the response displacements of inelastic structures depending on the spectral region. In adjacent inelastic structures, such as colliding buildings or interacting bridge segments, contact is likely to alter drastically the excitation frequencies' at which the system is most vulnerable. Finally, it is shown that the proposed approach yields maximum response displacements which correlate very well with the persistency of real earthquakes for a bridge system with considerably complex behaviour.

Keywords Pounding · Unilateral contact · Earthquake engineering · Non-linear structural dynamics dimensional analysis · Bridges

E. G. Dimitrakopoulos (✉)
Department of Engineering, University of Cambridge, Cambridge CB2 1 PZ, UK
e-mail: ilias.dimitrakopoulos@gmail.com

N. Makris
Department of Civil Engineering, University of Patras, 26500 Patras, Greece

A. J. Kappos
Department of Civil Engineering, Aristotle University of Thessaloniki, 54124 Thessaloniki, Greece

Abbreviations

DA	Dimensional Analysis
LCP	Linear Complementarity Problem
MSSS	Multi-Span Simply-Supported
PGA	Peak Ground Acceleration
SDOF	Single Degree Of Freedom

1 Introduction

This paper derives from a broader study (Dimitrakopoulos et al. 2009a,b; Dimitrakopoulos et al. 2010; Dimitrakopoulos 2010) on the dynamics of pounding between adjacent structures due to earthquake shaking. The motivation for the work reported herein, is the need to elucidate the earthquake response of the pounding bridge segments. This is attempted by bringing forward the fundamental physical similarities that govern the response of such multi-parametric mechanical systems with the aid of formal dimensional analysis (DA) (Barenblatt 1996; Sedov 1992).

In 1995 Malhotra et al. (1995) presented the recorded seismic response of a bridge with joints, wherein sharp spikes in the acceleration records from the deck were attributed to in-deck pounding. Few years later, Malhotra (1998) made an analytical effort to comprehend the phenomenon of earthquake-induced pounding in bridges. He concluded that due to pounding, column forces as well as, the longitudinal separation at in-deck joints are reduced. His conclusions though, are conflicting those of Jankowski et al. (1998) who studied the impact of many SDOF oscillators in a row, in an effort to simulate the pounding induced by propagating seismic waves in multi-span isolated bridges.

Further studies on the impact of bridge segments have been presented by DesRoches and Muthukumar (2002) who examined the impact response of elastic and inelastic oscillators including the event of adjacent structures restrained with cables. That study concludes that when the natural frequency and the excitation frequency are separated the one-sided impact is accentuated, whereas impact suppresses the response of oscillators at resonance. At about the same time an analogous study was conducted in Japan by Ruangrassamee and Kawashima (2001) who considered pounding between two linear SDOF oscillators and proposed the so-called 'relative displacement response spectrum with pounding effect'.

Zanardo et al. (2002) considered the spatial variability of the earthquake excitation when studying the response of bridges with pounding. Saadeghvaziri et al. (2000) took into account the soil-structure interaction effects on the seismic response of multi-span simply-supported bridges (MSSS) with pounding phenomena. Dicleli (2008) focused on the ability of elastic gap devices to enhance the performance of pounding seismically isolated bridges under the influence of near-fault excitations. Further references on pounding oscillators can be found in Dimitrakopoulos et al. (2009a,b); Dimitrakopoulos et al. (2010).

The present study builds on the previous work of the authors (Dimitrakopoulos et al. 2009a,b; Dimitrakopoulos et al. 2010) which concerned elastic pounding structures and extends the proposed dimensional analysis approach to inelastic structures with inelastic pounding.

2 Proposed methodology

The methodology presented herein, is rather novel from two different aspects:

(i) In the vast majority of seismic engineering studies impact and contact phenomena are taken into account via a contact element. Herein, a different approach is adopted that stems from non-smooth dynamics. All physically feasible unilateral contact configurations (impacts, continuous contacts, and detachments) are mathematically treated as inequality problems, namely Linear Complementarity Problems (LCPs), according to multibody dynamics with unilateral contacts in the form presented by Leine et al. (2003).

(ii) On the other hand, in order to uncover the fundamental physical similarities that describe the pounding behaviour of bridges, formal dimensional analysis (DA) (Barenblatt 1996; Sedov 1992) is implemented. DA is a tool of mathematical physics that shapes the general form of relations that describe physical phenomena. When the behaviour of pounding structures is described in the dimensionless terms yielded from DA the non-linear, non-smooth response is liberated from the need to refer to a substitute system and the remarkable property of self-similarity, a special type of symmetry - invariance with respect to the intensity and the frequency content of the excitation, is revealed. In Dimitrakopoulos et al. (2009a,b); Dimitrakopoulos et al. (2010) it was shown that DA offers a lucid interpretation of the response of elastic pounding oscillators.

2.1 Time and length scales in earthquake records with distinct pulses

The application of the proposed (DA) method hinges upon a distinct time scale (ω_g) and a length scale $\left(a_g\right)$ that characterize the ground shaking and are relevant to structural response. In records with distinct pulses, such time and length scales emerge naturally from the distinguishable pulses which dominate a wide class of strong (usually near-field) earthquake records; they are directly related with the rise time and slip velocity of faulting. The minimum number of input parameters of such models is two and they have an unambiguous physical meaning. Herein the acceleration amplitude α_p $\left(a_g = a_p\right)$ and duration $T_p(\omega_g = 2\pi/T_p)$of the pulse are used. Fig. 1 (top) shows the time history from the 1995 Aegion (Greece) earthquake record, as well as the pulse duration T_p and the pulse acceleration α_p.

2.2 Time and length scales in earthquake records without distinct pulses

In many records, including typical Greek records, there are no distinct pulses (Fig. 1 bottom). Nevertheless, it is still feasible to apply the proposed (DA) approach provided the appropriate time and length scales are adopted. This is a critical issue of the proposed approach, which is treated in detail in Dimitrakopoulos et al. (2009a,b). In that study such scales, together with the associated selection criteria, are proposed among the available in literature strong ground-motion parameters. These are the peak ground acceleration ($a_g = PGA$) as length scale, and the mean period T_m (Rathje et al. 1998) as time scale ($\omega_g = 2\pi/\mathrm{T}_m$), where $T_m = \sum_i \left(C_i^2/f_i\right)/\sum_i C_i^2$, C_i are the Fourier amplitudes of the accelerogram and f_i the discrete Fourier transform frequencies between 0.25 and 20 Hz. It is recalled here, that when the focus is on a peak response parameter, it is the frequency content and not the duration of an excitation that is of interest (see Dimitrakopoulos et al. (2009a,b) and references therein). When the response is described in dimensionless terms that hinge upon those parameters (PGA, T_m), the remarkable order of self-similarity emerges. In addition, this approach reduces drastically the scatter in the response of some fundamental mechanical configurations of earthquake engineering (Dimitrakopoulos et al. 2009a,b): the

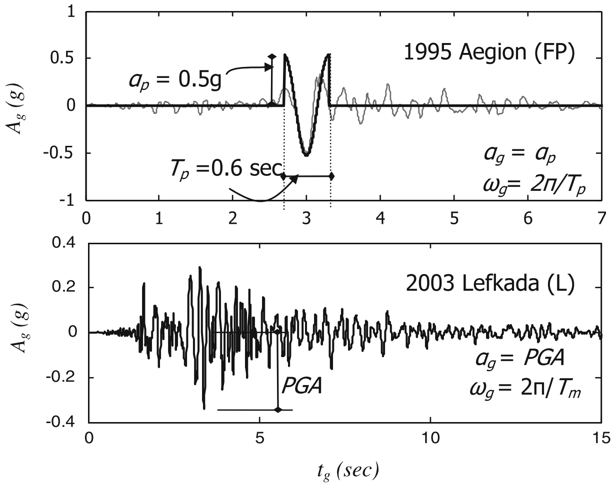

Fig. 1 Time and Length Scales in earthquake records with (*top*) and without (*bottom*) distinct pulses

elastic-plastic system and the pounding oscillator. Herein the same approach is extended to inelastic structures with inelastic pounding.

3 Dimensional analysis of an elasto-plastic pounding system

In general, the equation of motion of an inelastic SDOF oscillator, subjected to base excitation and taking into account contact phenomena can be written as:

$$m\ddot{u}(t) + F_{\text{int}}(t) - W \cdot \lambda(t) = -m\ddot{u}_g(t) \tag{1}$$

where u is the relative, to the ground, response displacement, u_g is the ground displacement, m the mass, and F_{int}, the internal inelastic force of the oscillator. W is the direction vector of the constraint (contact) force λ which herein is considered as a Lagrange multiplier, see also Dimitrakopoulos et al. (2009a,b).

In case of elasto-plastic behaviour the internal inelastic force F_{int} is given by:

$$\frac{F_{\text{int}}(t)}{m} = 2\xi\omega_s \cdot \dot{u}(t) + \frac{Q}{m} \cdot z(t) \tag{2}$$

where ξ is the damping ratio, ω_s the angular frequency of the structure after yielding (post-yielding), Q the specific strength of the structure and z is a dimensionless hysteretic parameter, with $|z| \leq 1$, that is given by:

$$\dot{z}(t) = \frac{1}{u_y}\left[\dot{u}(t) - \gamma\,|\dot{u}(t)|\,z \cdot |z|^{n-1} - \beta\dot{u}(t)\,|z|^n\right] \tag{3}$$

Equation (3) is a special case of the Bouc-Wen model (Wen 1975, 1976) that has been used extensively for simulating seismic isolation systems (Makris and Chang 2000). Parameters β, γ, and n are dimensionless quantities that shape the hysteretic loop and herein are taken as: $\beta = \gamma = 0.5$ and $n = 20$ (Makris and Chang 2000).

Substituting Eq. (2) into the equation of motion (1) yields:

$$\ddot{u}(t) + 2\xi\omega_s \cdot \dot{u}(t) + (Q/m) \cdot z(t) - (1/m) \cdot W \cdot \lambda(t) = -\ddot{u}_g(t) \tag{4}$$

Conclusively, the parameters necessary to determine a response quantity of an elasto-plastic pounding oscillator subjected to ground excitation, e.g. the maximum response displacement u_{max} are: u_y the yield displacement and Q/m the characteristic strength, the acceleration amplitude α_g and the angular frequency of the excitation ω_g (Fig. 1), the initial distance between the oscillator and the rigid barrier "gap" δ, and the coefficient of restitution ε_{N}. Assuming a pure hysteretic behaviour (zero viscous damping $\xi = 0$) the response function can be written as:

$$u_{\max} = f(u_y, Q/m, \delta, \varepsilon_N, a_g, \omega_g) \tag{5}$$

This results in a group of 7 variables which involve only 2 reference dimensions, those of length [L] and time [T]. According to Buckingham's "Π" theorem the number of independent dimensionless Π-products is now: (7 variables) − (2 reference dimensions) = 5 Π-terms.

Herein, the characteristics of the excitation, α_g and ω_g are selected in order to normalise the non-linear response (including both yielding and pounding) to the energetic length scale of the excitation, $L_e = \alpha_g/\omega_g^2$ The product α_g/ω_g^2 is a characteristic length scale of the (ground) excitation's persistence to impose deformation demands, see for instance Dimitrakopoulos et al. (2009a,b) and references therein. Accordingly, Eq. (5) reduces to:

$$\frac{u_{\max}\omega_g^2}{a_g} = \phi\left(\frac{\delta\omega_g^2}{a_g}, \varepsilon_N, \frac{u_y\omega_g^2}{a_g}, \frac{Q}{ma_g}\right) \tag{6}$$

or

$$\Pi_{\mathrm{um}} = \phi(\Pi_\delta, \Pi_\varepsilon, \Pi_{\mathrm{uy}}, \Pi_{\mathrm{Q}}) \tag{7}$$

with:

$$\Pi_{\mathrm{um}} = \frac{u_{\max}\omega_g^2}{a_g}, \Pi_\delta = \frac{\delta\omega_g^2}{a_g}, \Pi_\varepsilon = \varepsilon_N, \Pi_{\mathrm{uy}} = \frac{u_y\omega_g^2}{a_g}, \Pi_{\mathrm{Q}} = \frac{Q}{ma_g} \tag{8}$$

The dependent variable, dimensionless product Π_{um}, is the maximum response displacement normalized to L_e. The dimensionless gap Π_δ and the coefficient of restitution ε_{N} are the pounding parameters, whereas the dimensionless yield displacement Π_{uy} and the characteristic strength Π_{Q} are associated with the elasto-plastic behaviour of the structure. The dimensionless gap $\Pi_\delta = \delta\omega_g^2/\alpha_g$ and the dimensionless yield displacement $\Pi_{\mathrm{uy}} = u_y\omega_g^2/\alpha_g$ are novel intensity measures which suggest that the size of the gap "δ" and the yield displacement u_y accordingly, can be scaled to the energetic length scale $L_e = \alpha_g/\omega_g^2$ [m] (Dimitrakopoulos et al. 2009a,b). In contrast to other intensity measures proposed recently in the literature (Vega et al. 2009), Π_δ and Π_{uy} are rationally produced and dimensionally consistent intensity measures which as illustrated later on, correlate well with the response of such mechanical configurations.

Figure 2 presents the response spectra of an elasto-plastic pounding system to a cosine pulse, for different excitation intensities. The most decisive feature of the proposed DA approach (dimensionless terms Π_δ and Π_{uy}) is that it brings forward the property of self-similarity even when the two different types of non-linearity coexist, i.e. the unilateral contact phenomena and the inelastic behaviour of the structure itself. The response curves expressed in the Π-terms for different intensity and frequency of the excitation follow a master-curve (self-similarity—Fig. 2 right)

Figure 3 presents simultaneously the two key parameters of the proposed approach: the dimensionless gap $\Pi_\delta = \delta\omega_g^2/\alpha_g$ and the dimensionless yield displacement $\Pi_{\mathrm{uy}} = u_y\omega_g^2/\alpha_g$. Figure 3 left plots contours of Π_δ on the plane: $(\delta) - (1/L_e)$ for several types of bridges and

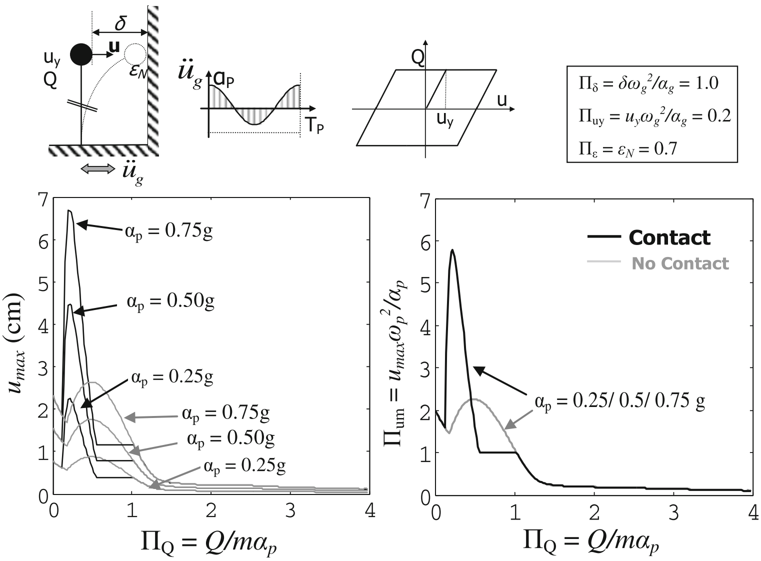

Fig. 2 The response spectra for different excitation intensities and a given dimensionless gap Π_δ, and yield displacement Π_{uy} (*left*) collapse to a single curve (self-similarity) when expressed in the proposed dimensionless Π-terms (*right*)

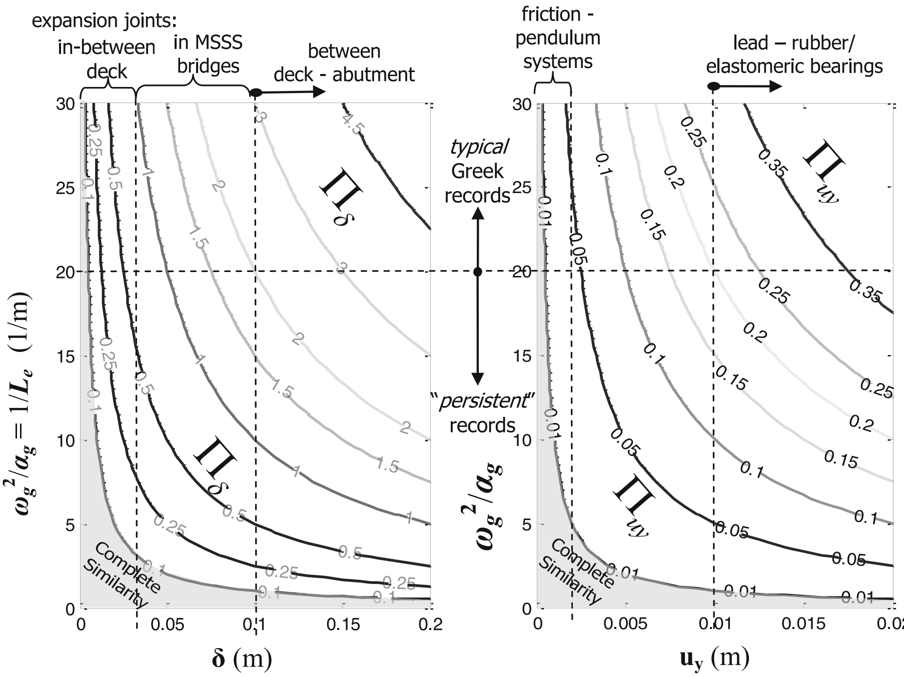

Fig. 3 *Left*: Contours of dimensionless gap $\Pi_\delta = \delta\omega_g^2/\alpha_g$ values, for several bridge types and earthquakes. *Right*: Contours of dimensionless yield displacement $\Pi_{\mathrm{uy}} = u_y\omega_g^2/\alpha_g$ values, for several seismic isolation types and earthquakes. The vertical axis in both diagrams scales the inverse of the earthquake's persistency $(1/L_e = \omega_g^2/\alpha_g)$

earthquakes. Typical values of in-deck expansion joints range from 0.6 to 1.3 cm (DesRoches and Muthukumar 2002), in MSSS bridges (Saadeghvaziri and Yazdanimotlagh 2008) from 2.5 to 7.5 cm while larger values are common in deck-abutment expansion joints. Figure 3 (right) plots contours of Π_{uy} on the plane: $(u_y) - (1/L_e)$ for several seismic isolation types. Representative values of u_y for each seismic isolation type are drawn from Makris and Black (2004a). The vertical axis is common for both diagrams (left and right) of Fig. 3 and scales the inverse of the excitation's persistency $(1/L_e = \omega_g^2/\alpha_g)$. Greek earthquakes records are systematically less persistent (Fig. 3) than popular earthquakes records as for instance the ones considered in Makris and Psychogios (2006). As a consequence, the same gap size δ corresponds to a smaller dimensionless gap Π_δ when the bridge is subjected to an earthquake like San Fernando (1971) (Makris and Psychogios 2006) than to an earthquake like Lefkada 2003 (Fig. 1 bottom).

The shaded areas, in both diagrams under the contour Π_δ=0.1(and $\Pi_{uy} = 0.1$ accordingly) correspond to the area where complete similarity prevails. The property of complete similarity reveals that the response of a pounding oscillator is indifferent to small values of the dimensionless gap ($\Pi_\delta < 0.1$) (Dimitrakopoulos et al. 2010) and that the response of an elasto-plastic system is indifferent to small values of the dimensionless yield displacement ($\Pi_{uy} < 0.1$) (Makris and Black 2004b) accordingly. For instance, if the dimensionless yield displacement Π_{uy} turns out small enough ($\Pi_{uy} < 0.1$) the engineer can expect that the initial pre-yielding stiffness may be immaterial to the actual response of the structure (Makris and Black 2004b). What is also evident from Fig. 3 is the similar way that dimensionless terms Π_δ and Π_{uy} depend on the earthquake's persistency. Thus, the estimation of the dimensionless terms describing the response (e.g. Π_δ and Π_{uy} after evaluating L_e) may provide, through diagrams like Fig. 3, information on the sensitivity of the structure to phenomena like yielding or pounding before an analysis is performed.

Figure 4 illustrates the response spectra for a given dimensionless yield displacement ($\Pi_{uy} = 0.2$) and several dimensionless gaps Π_δ, of an elasto-plastic SDOF oscillator subjected to pulse-type excitations. The response spectra of Fig. 4 are self-similar; they are indifferent to the excitation's intensity and period. Similar results are obtained for several dimensionless yield displacements e.g. $\Pi_{uy} = 0.01$, even though they are not presented herein for economy of space. Self-similarity is a well-known property of linear elastic response, hence response curves for the no-contact case (grey lines in Fig. 4) illustrate the same feature.

The accentuation of the response, due to contact, is intense in the area of weak systems/short pulses (small Π_Q values). The opposite holds true for intermediate Π_Q values, the response diminishes due to contact. In addition, in the area of strong systems/ long pulses (high Π_Q values) the maximum response displacement is indifferent to contact. Consequently, three distinct spectral areas are recognized in the response, which appear systematically for inelastic as well as linear elastic pounding oscillators (Dimitrakopoulos et al. 2009a,b). Compared with the bilinear behaviour (Fig. 5), the accentuation of the response due to contact is more pronounced in the case of elasto-plastic behaviour, which is attributed to the (comparatively) lower restoring force.

The examined mechanical configuration lacks symmetry with respect to the direction (normal/reverse) of motion. Left and right columns of Fig. 4 differ only in the directivity of the pulse and reflect this peculiarity. Differences in the response are more pronounced for excitations with a strong "preference" in a specific direction like sine pulses, which represent pure forward motions. The directivity effects wear off for excitations with more loading cycles and/or no preference to a specific direction. In modern literature lack of symmetry in configurations of pounding structures is often quite disregarded with the risk of loosing valuable information (Dimitrakopoulos et al. 2010).

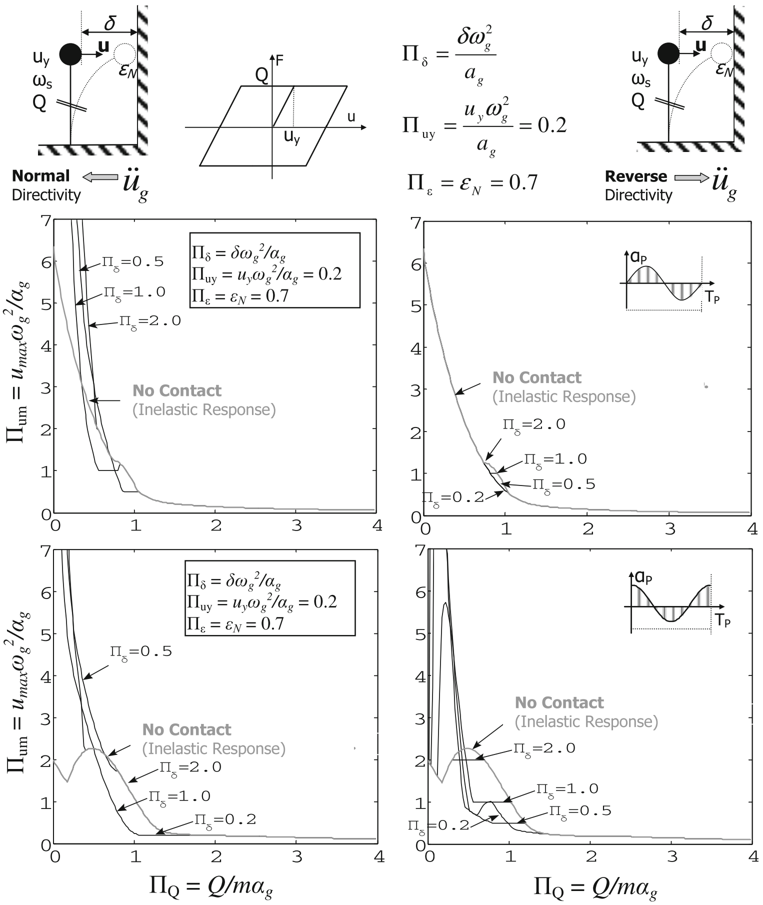

Fig. 4 Self-similar response spectra of the elasto-plastic pounding system, subjected to pulse-type excitations of normal (*left*) and reverse (*right*) directivity

Depending on the excitation's shape and directivity, response may be very sensitive to moderate and high dimensionless gap values (Fig. 4). However, for small enough dimensionless gaps ($\Pi_\delta < 0.5$) the response displacement is indifferent to Π_δ. This invariance of the response for small Π_δ values confirms the existence of the complete similarity region (grey area) in Fig. 3 for inelastic structures, originally observed for the elastic pounding oscillator (Dimitrakopoulos et al. 2010).

4 Dimensional analysis of a bilinear sdof pounding oscillator

Before moving on to bilinear pounding structures, it is useful to revisit first inelastic structures without pounding. The dynamic equilibrium of a bilinear SDOF oscillator with mass m that is subjected to a ground excitation gives:

$$\ddot{u}(t) + \frac{F_{\text{int}}(t)}{m} = -\ddot{u}_g(t) \tag{9}$$

with the same notations as in Eq. (1).

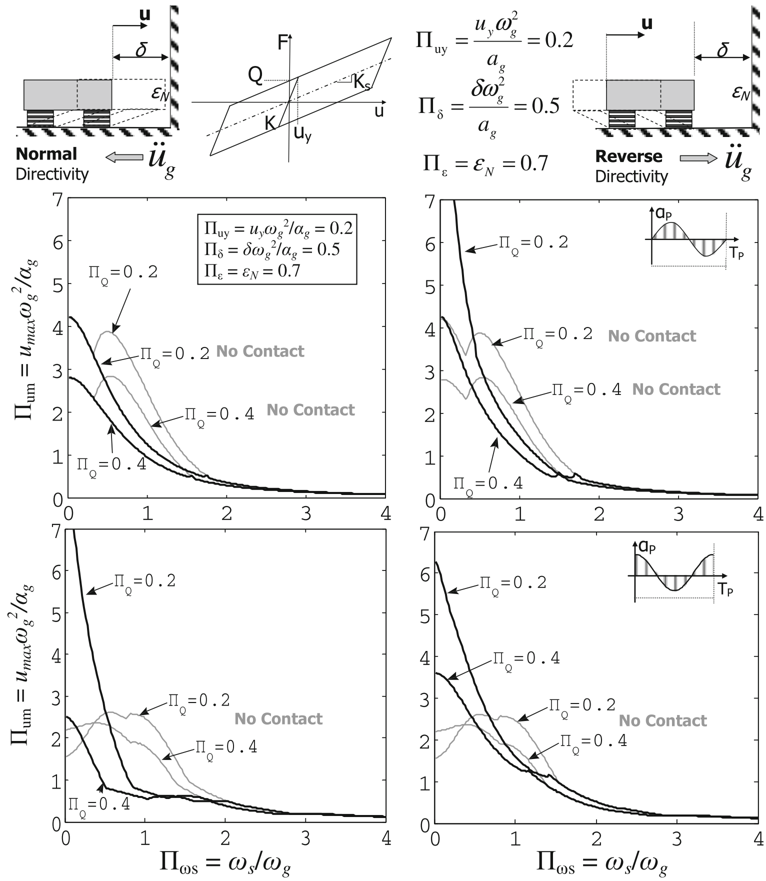

Fig. 5 Self-similar response spectra of a bilinear pounding structure, subjected to pulse-type excitations of normal (*left*) and reverse (*right*) directivity

A bilinear hysteretic loop (Fig. 5 top) can de defined with an appropriate combination of three of the following parameters: characteristic strength Q, yield force F_y, pre-yielding stiffness K_0, post-yielding stiffness (second slope of the bilinear loop) K_s, hardening $\alpha = K_s/K_0$, and yield displacement u_y. Consequently, there is no unique way, but depending on the adopted parameters, several alternative ways of describing a structure with bilinear behaviour.

Seismically isolated structures are designed intentionally with small yield displacements and/or strength in order to perform inelastically when subjected to the design earthquake. Makris and Black (2004a), expressed the response of isolated structures with the triplet: Q(or Q/m), u_y and ω_s(or T_s), and revealed the remarkable property of complete similarity with respect to small dimensionless yield displacements Π_{uy}. This property unveils that the elastic characteristics of structures designed with small yield displacements are indifferent to the (essentially inelastic) response. The response function of a bilinear SDOF pounding oscillator (Fig. 5 bottom), when the inelastic behaviour is described with the triplet (Q or Q/m, u_y and ω_s or T_s), can be written as:

$$u_{\max} = f\left(\omega_s, \frac{Q}{m}, u_y, \delta, \varepsilon_N, a_g, \omega_g\right) \tag{10}$$

and by following an analogous analysis, the relation of the dimensionless Π-terms is:

$$\Pi_{\text{um}} = \phi(\Pi_{\omega s}, \Pi_\delta, \Pi_\varepsilon, \Pi_{\text{uy}}, \Pi_{\text{Q}}) \tag{11}$$

with:

$$\Pi_{\omega s} = \frac{\omega_s}{\omega_g}, \Pi_{\text{Q}} = \frac{Q}{ma_g} \tag{12}$$

and the remaining Π-terms are as in Eq. (8).

Figure 5 presents the same results as Fig. 4, but for a bilinear instead of elasto-plastic, pounding SDOF system. The bilinear behaviour is described in terms of the dimensionless $\Pi_{\omega_\text{s}} = \omega_s/\omega_g$ while the elasto-plastic behaviour is expressed in terms of $\Pi_\text{Q} = Q/m\alpha_g$ and appears as the limit case of the bilinear one for $\Pi_{\omega_\text{s}} = 0$ The self-similar response spectra of Fig. 5 illustrate the same trends (as Fig. 4) regarding the influence of contact.

Figure 6 plots the self-similar response spectra of an SDOF pounding oscillator with elastic (top), elasto-plastic (middle) and bilinear (bottom) behaviour. In all three cases the dimensionless gap Π_δ, the coefficient of restitution ε_N and the excitation are the same. The dimensionless approach proposed herein unveils the property of self-similarity in all cases considered, even though the response is strongly non-linear (non-smooth) due to contact as well as inelastic (elasto-plastic or bilinear). What is also noteworthy about Fig. 6 is the qualitatively similar way in which contact influences the structural response. Whether the structural response is elastic, elasto-plastic or bilinear, the spectrum shape resembles an asymptotic (exponential) form and the aforementioned three spectral areas appear. In other words, when the dimensionless gap is small enough, contact alters the response up to the point that it overshadows its original characteristics.

5 Multiple inelastic pounding oscillators

In the general case, a mechanical configuration of n bilinear SDOF oscillators in a row is governed by $4n + 4$ variables. These are:

- ω_{si}, u_{yi}, Q_i, and m_i, and m_i: the post-yielding angular frequency, the yield displacement, the characteristic strength and the mass of the oscillator with index i, where $i = 0 \div n - 1$. In the following, the oscillator under examination is denoted with sub-index 0 and the equivalent viscous damping ratio of the oscillators is ignored ($\xi = 0$).
- ε_N and δ: the coefficient of restitution and the gap.
- a_g and ω_g: a characteristic length and time scale of the excitation (Fig. 1)

Hence a response quantity of interest, e.g. the maximum response displacement u_{max}, of an oscillator, can be written as a function of the general form:

$$u_{\max} = f\left(\omega_{si}, Q_i, m_i, u_{yi}, \delta, \varepsilon_N, a_g, \omega_g\right), i = 0 \div n - 1 \tag{13}$$

This results in a set of 4n + 5 variables which involve 3 reference dimensions, those of length [L], time [T] and mass [M]. According to Buckingham's "Π" theorem the number of independent dimensionless Π-products is now: ($4n + 5$ variables) – (3 reference dimensions) $= 4n + 2$Π-terms.

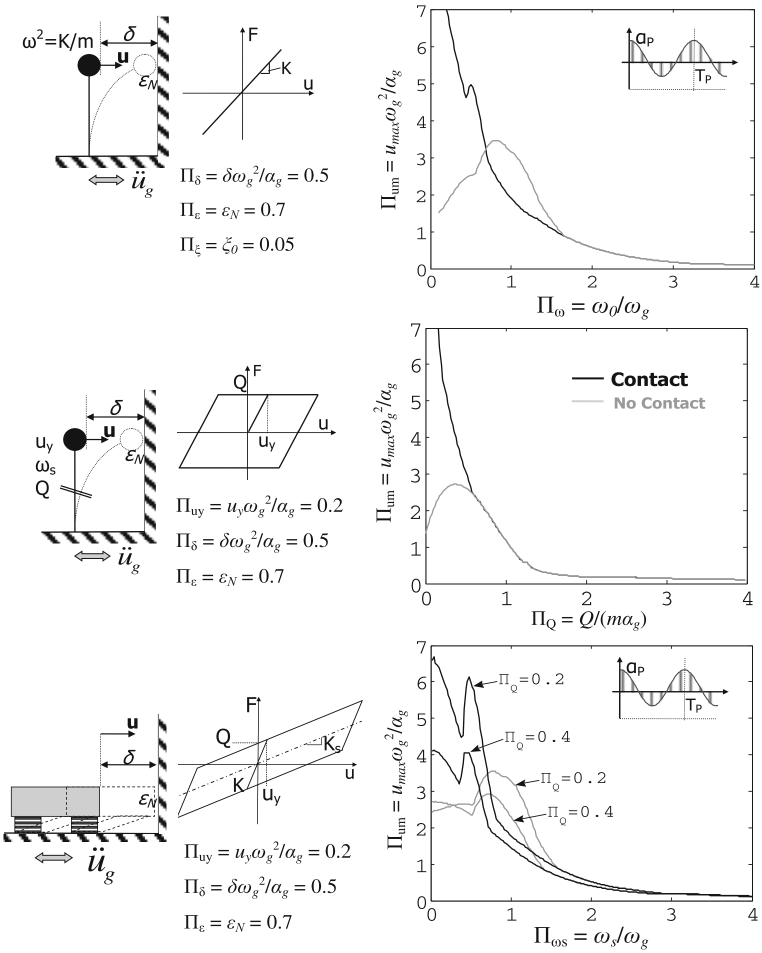

Fig. 6 Response spectra of a SDOF pounding oscillator. elastic (*top*), elasto-plastic (*middle*) and bilinear (*bottom*)

Extending the same approach, the characteristics of the excitation, α_g and ω_g, and the properties of a reference-oscillator (ω_0 and m_0) are selected as repeating variables. Accordingly, Eq. (5) reduces to:

$$\frac{u_{\max}\omega_g^2}{a_g} = \phi\left(\frac{\delta\omega_g^2}{a_g}, \varepsilon_N, \frac{\omega_{s0}}{\omega_g}, \frac{u_{y0}\omega_g^2}{a_g}, \frac{Q_0}{m_0 a_p}, \frac{m_0}{m_i}, \frac{\omega_{s0}}{\omega_{si}}, \frac{u_{yi}\omega_g^2}{a_g}, \frac{Q_i}{m_i a_g}\right), \quad i = 1 \div n-1 \tag{14}$$

or

$$\Pi_{\text{um}} = \phi(\Pi_\delta, \Pi_\varepsilon, \Pi_{\omega s0}, \Pi_{\text{uy0}}, \Pi_{\text{Q0}}, \Pi_{\text{mi}}, \Pi_{\text{si}}, \Pi_{\text{uyi}}, \Pi_{\text{Qi}}), \quad i = 1 \div n-1 \tag{15}$$

with:

$$\Pi_{\omega s0} = \frac{\omega_{s0}}{\omega_g}, \Pi_{\text{si}} = \frac{\omega_{\text{s0}}}{\omega_{\text{si}}}, \Pi_{\text{mi}} = \frac{m_0}{m_i} \tag{16}$$

and the remaining Π-terms as in Eq. (8).

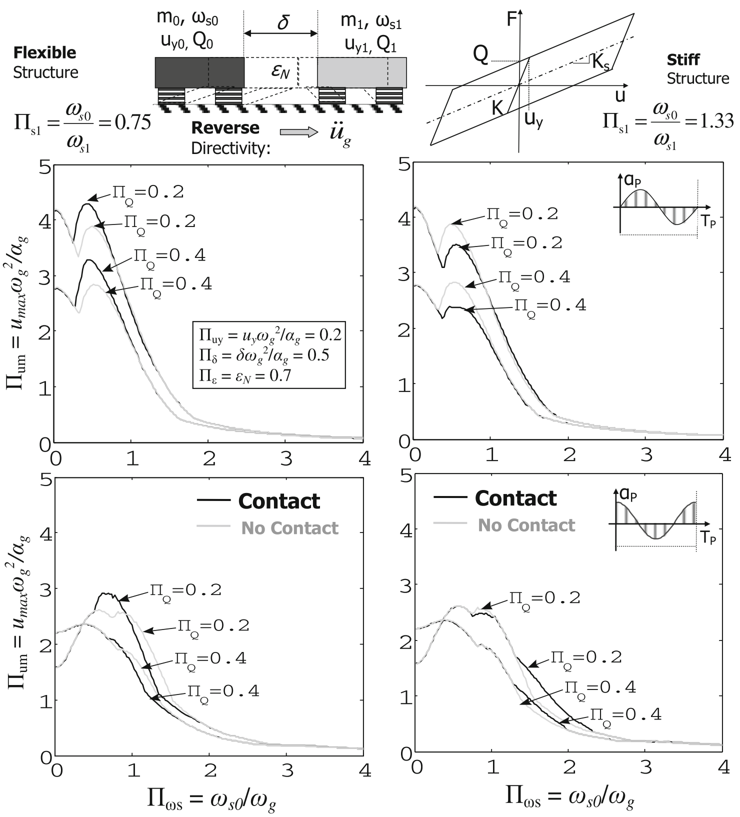

Fig. 7 Self-similar response spectra of a pair of bilinear pounding structures, subjected to pulse-type excitations. Left column corresponds to most flexible and right column to most stiff among a pair of structures

Eq. (14) shows that 10 Π-terms govern the problem of a pair ($n = 2$) of bilinear SDOF structures (Fig. 7) and 14Π-terms the response of three ($n = 3$) bilinear structures in a row (Figs. 8 and 9). Thus, Eq. (14) clearly illustrates the multiparametric nature of the dynamics of pounding-structures.

For convenience, simplifying assumptions are made in the following parametric study. It is assumed that the mass, strength and yield displacement of the structures examined are the same: $m_0 = m_i$, $Q_0 = Q_i$, $u_{y0} = u_{yi}$. Under these rather restrictive assumptions Fig. 7 plots the response spectra of a structure (with characteristics: ω_0, m_0, u_{y0} and Q_0) involved in a pair of bilinear structures. Figures 8 and 9 present the same results as Fig. 7 but for the centric structure, from a symmetric triplet of bilinear pounding structures. Left columns (of Figs. 7, 8, 9) present the response of the more flexible structure of the system considered ($\Pi_{s1} < 1$), while right columns present the response of the stiffer structure ($\Pi_{s1} > 1$).

As the (post-yielding) angular frequencies of the structures separate, the influence of contact becomes more pronounced (compare Fig. 8 with 9), in agreement with the pertinent conclusions of DesRoches and Muthukumar (2002). It is reminded though, that this is true provided the masses of the colliding structures are the same. A more detailed analysis of the role of the mass ratio shows that when masses differ substantially contact may alter

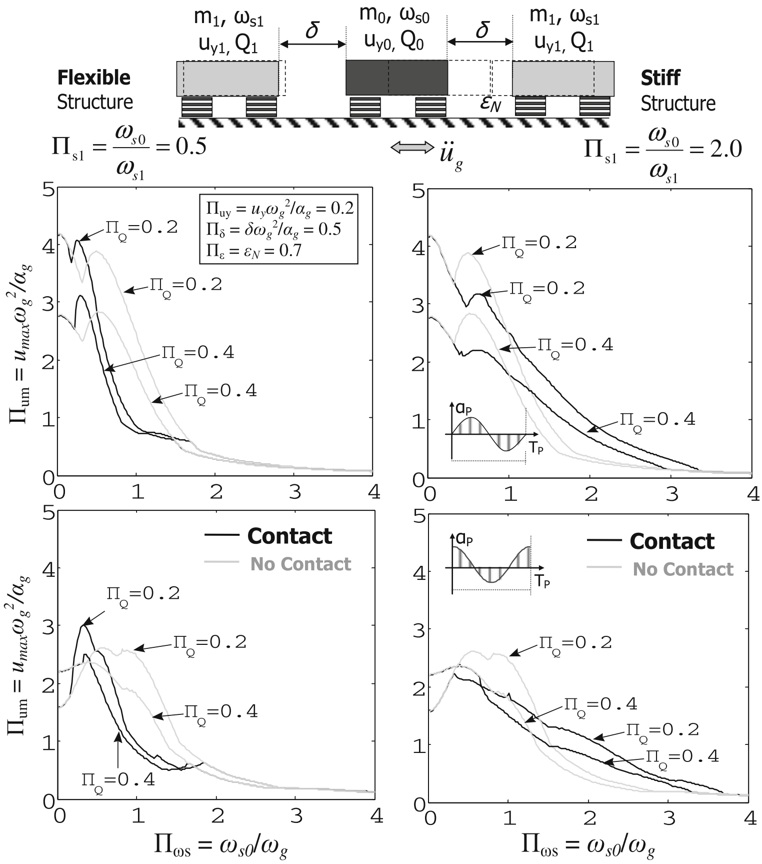

Fig. 8 Self-similar response spectra of a symmetric triplet of bilinear pounding structures, subjected to pulse-type excitations. Left column corresponds to most flexible and right column to most stiff structure

drastically the response of linear pounding oscillators even if structural frequencies are similar (Dimitrakopoulos et al. 2009a,b).

As a result of contact, the shape of the spectrum of a flexible structure sharpens, while that of a stiff structure flattens. This characteristic is associated with the three spectral regions, previously noted for single pounding structures, which arise also for the considered systems of multiple pounding structures. The difference is that the response of flexible structures is accentuated in the area of short pulses (small $\Pi_{\omega s}$), while the response of stiff structures is accentuated in the area of long pulses. For $\Pi_{\omega s}$ near unity the maximum response displacement usually diminishes for all structures. A collateral consequence is that in adjacent inelastic structures, such as individual deck segments or neighbouring buildings, contact alters the frequencies which stimulate the most the individual parts of the system compared with the no-contact dynamic behaviour. For instance when a structure is excited near its effective (post-yielding) frequency its response may be hindered due to contact, but at the same time the response of their neighbouring structure is often accentuated. This is a critical trend from a practical point of view, observed also in linear pounding oscillators (Dimitrakopoulos et al. 2009a,b), since contact alters the excitation frequencies' at which such mechanical configurations are most vulnerable.

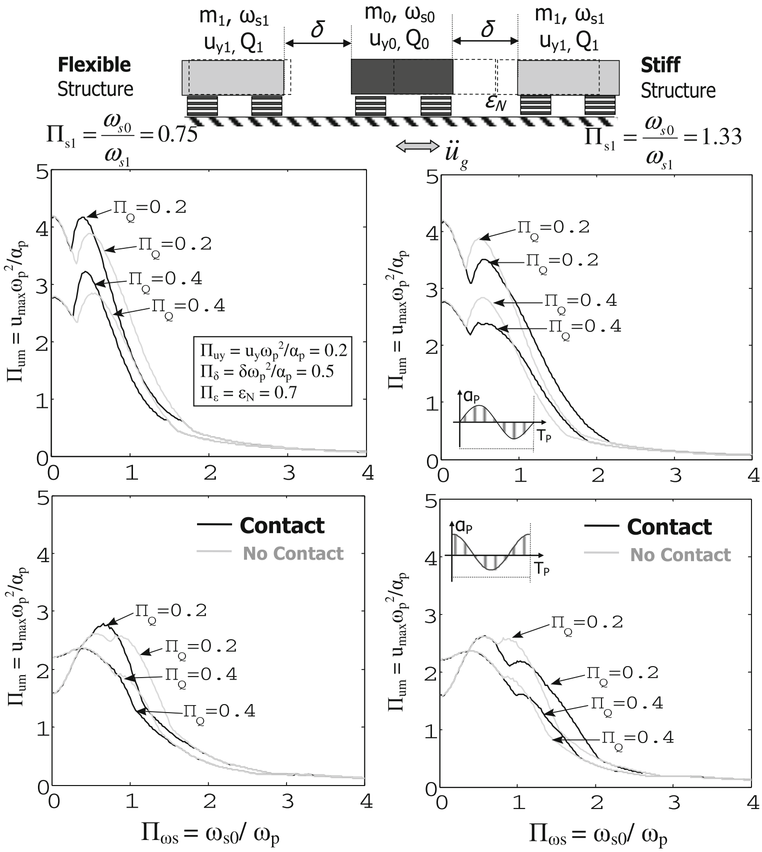

Fig. 9 Self-similar response spectra of a symmetric triplet of bilinear pounding structures, subjected to pulse-type excitations. Left column corresponds to most flexible and right column to most stiff structure

The proposed dimensionless spectra (Figs. 7, 8, 9) are self-similar, i.e. (for given values of the associated Π-terms) are indifferent to the intensity of the excitation. Self-similarity is of unique importance since it reveals invariance with respect to scale transformations (intensity of the excitation). At the same time, traditional response spectra, useful for spectrum-based design, can be calculated from the proposed spectra through a simple similarity transformation.

6 Illustrative example

The proposed methodology is implemented on a two-segment frame bridge (Fig. 10) with the characteristics presented in Table 1, similar with those in DesRoches and Muthukumar (2002).

The equation of motion for the bridge system examined, taking into account unilateral contact can be written as:

$$\mathbf{M}\ddot{\mathbf{u}} + \mathbf{F}_F(\mathbf{u}) - \mathbf{F}_B(\mathbf{u}_j - \mathbf{u}_i) - \mathbf{W}\lambda = -\mathbf{M}\delta\ddot{u}_g \tag{17}$$

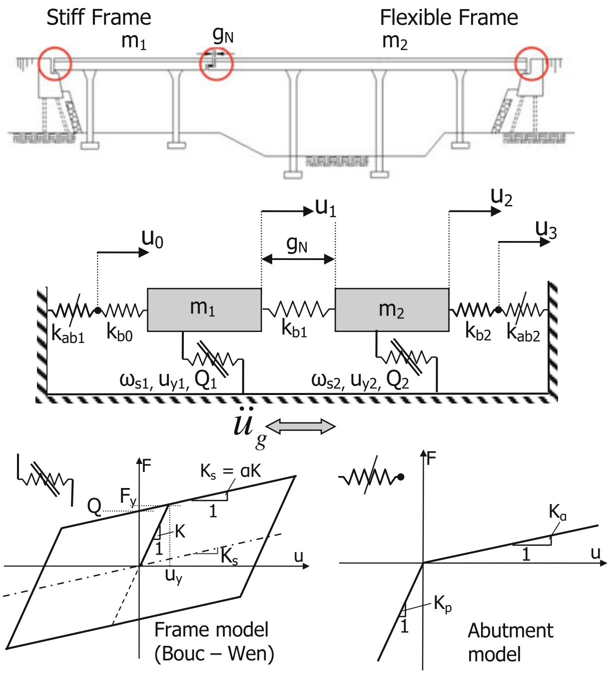

Fig. 10 *Top*: Layout of the bridge examined. *Middle*: Mechanical model of the bridge system and parameters involved. *Bottom*: non-linear elements of the model

Where the mass matrix is: $\mathbf{M} = diag\,\{m_1\; m_2\}$, λ is the contact force considered as a Lagrange multiplier (see also Dimitrakopoulos et al. (2009a,b), $\boldsymbol{\delta}$ is the unit vector and **W** the direction vector. The restoring characteristics ($\mathbf{F}_F$) of the two segments of the bridge are modelled with pertinent bilinear hysteretic Bouc-Wen springs (Fig. 10—bottom left):

$$\mathbf{F}_F(\mathbf{u}) = \begin{bmatrix} F_{F1}(u_1) \\ F_{F2}(u_2) \end{bmatrix} = \begin{bmatrix} k_{s1}u_1(t) + Q_{s1}z_{s1}(t) \\ k_{s2}u_2(t) + Q_{s2}z_{s2}(t) \end{bmatrix} \tag{18}$$

where k_s denotes the post-yielding stiffness, Q_s the specific strength and z the dimensionless hysteretic parameter, governed by Eq. (3). A $\xi = 5\%$ viscous damping ratio and a coefficient of restitution $\varepsilon_N = 0.7$ is assumed.

Table 1 Characteristics of the bridge examined

Element	Initial stif. (kN/m)	Yield str (kN)	Period (s)	Strain hardening	Weight (t)
Frame – F_1	2,33,443	3,621	0.47	5%	1,301
Frame – F_2	1,01,048	3,794	1.12	5%	3,210
Element	Effective stif. (kN/m)	Element	Active stif. (kN/m)	Passive stif. (kN/m)	
Bearing – B_1	1,051	Abutment A_1, A_2	1,751	4,55,328	
Bearing B_0, B_2	1,50,000				

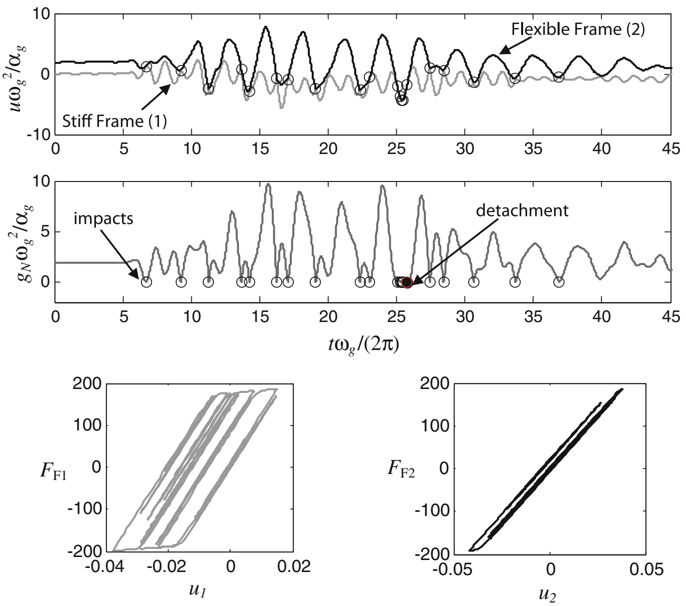

Fig. 11 Earthquake response analysis for the Lefkada 2003 record (shown in Fig. 1 *bottom*). Time histories in dimensionless terms: of the displacements of the two segments illustrating their relative distance g_N (*top*) and their relative distance g_N (middle). *Bottom*: the force—displacement loops of the two segments

The bearings are modelled using linear springs approximating their effective stiffness ($\mathbf{F}_B$):

$$\mathbf{F}_B(\mathbf{u}) = \begin{bmatrix} F_{B1}(u_2 - u_1) - F_{B0}(u_1 - u_0) \\ F_{B2}(u_3 - u_2) - F_{B1}(u_2 - u_1) \end{bmatrix} = \begin{bmatrix} k_{b1}(u_2 - u_1) - k_{b0}(u_1 - u_0) \\ k_{b2}(u_3 - u_2) - k_{b1}(u_2 - u_1) \end{bmatrix} \quad (19)$$

The behaviour of the abutments is assumed to follow the elastic bilinear spring ($\mathbf{F}_A$) shown in Fig. 10 (bottom right).

The bridge of Fig. 10 is analysed for the 62 Greeck records considered in Dimitrakopoulos et al. (2009a,b), comprising practically most of the available historic Greek records, without reference to any substitute pulses. Instead, all records are characterised directly using $\alpha_g = PGA$ and $\omega_g = 2\pi/T_m$, where T_m is the mean period (Rathje et al. 1998). With the aforementioned scales the notion of persistency or energetic length scale $L_e = \alpha_g/\omega_g^2$ [m] is extended to excitations with or without distinct pulses.

Sample results of the earthquake response analyses are offered in Fig. 11 for the Lefkada 2003 record of Fig. 1-bottom. In Fig. 11 open circles denote impacts, while filled circles denote the end of a continuous contact (detachment). The at-rest size of the joint between the two segments is: $\delta = 1.27$ cm, hence the dimensionless gap term for (typical) Greek records (Dimitrakopoulos et al. 2009a,b) is estimated as $\Pi_\delta = \delta\omega_g^2/\alpha_g > 0.5$. Similarly, the yield displacement of the two segments is accordingly $u_{y1} = 0.016$ and u_{y2} =0.038 m, so the dimensionless yield displacements are respectively greater than $\Pi_{uy1} = u_{y1}\omega_g^2/\alpha_g > 0.5$ and $\Pi_{uy2} > 1.2$.

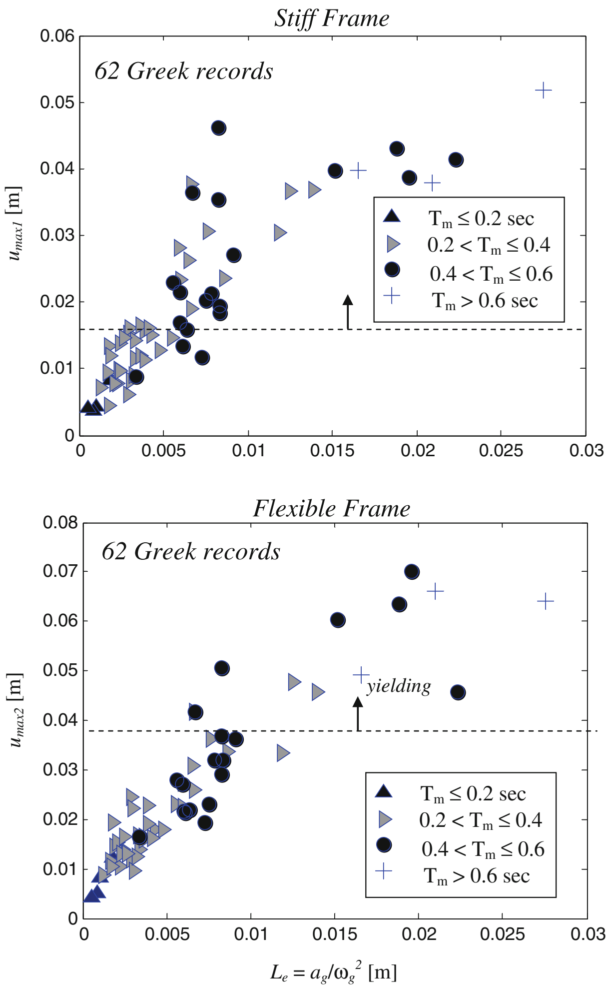

Fig. 12 Maximum response displacement of the stiff (*top*) and the flexible frame (*bottom*) vs. the energetic length scale of 62 Greek records (Dimitrakopoulos et al. 2009a,b)

The results from the 62 records (Fig. 12) reveal a strong correlation between the energetic length scale L_e (persistency) of (real) excitations with the maximum response displacement u_{max}. This is true, despite the complexity of the system's behaviour and the fact that two excitations with the same α_g and ω_g may differ substantially in (the accelerogram) shape which inevitably introduces a scatter in the response. For comparison, all excitations are grouped into 4 sets depending on their mean period T_m (Dimitrakopoulos et al. 2009a,b). Even though (mean) periods as well as the peak ground acceleration of each record may differ substantially, the response scales well with persistency L_e. Thus, the proposed DA approach verifies that what matters in the response of even more complex mechanical configurations are the dimensionless intensity measures, dimensionless gap Π_δ and yield displacement Π_{uy} values, and consequently the persistency of the excitation L_e. At the same time, plots like Fig. 12 can be useful, from a practical standpoint, in the same sense that traditional incremental dynamic analysis curves are.

7 Conclusions

The present paper proposes a novel, alternative way to describe the behaviour of pounding inelastic structures by implementing formal dimensional analysis in an effort to identify distinct physical similarities. Pounding structures comprise multi-parametric mechanical systems with quite complex earthquake response for which conflicting conclusions have been published in literature.

The application of the proposed method hinges upon the notion of persistency, or energetic length scale, of an excitation that assesses the tendency of ground shaking to impose deformation demands. The concept of persistency which is defined for excitations with or without distinct pulses is exploited herein to scale the response via meaningful new dimensionless intensity measures. The proposed approach leads to a condensed presentation of the response and most importantly unveils the remarkable property of self-similarity even though two different types of non-linearity coexist in the response: the boundary non-linearity of unilateral contact and the inelastic behaviour of the structure itself. It is shown that when the response is expressed in the appropriate dimensionless Π-terms, response spectra for any intensity and frequency content of the excitation collapse to a single master curve (self-similarity).

All physically realizable contact types are captured via a non-smooth complementarity approach. The present analysis also concludes that contact may have a different effect on the response displacements of inelastic structures depending on the structural and excitation's frequency ratio (spectral region). As for linear pounding oscillators, three distinct spectral regions are identified herein for inelastic pounding structures. The study also confirms that in adjacent inelastic structures, such as colliding buildings or interacting bridge segments, contact is likely to alter drastically the excitation frequencies at which the system is most vulnerable. Most often, contact results in amplifying the response of the most flexible, among pounding structures, in the low range of the frequency spectrum and the response of the most stiff structure in the upper range of the frequency spectrum.

Finally, the study concludes that the proposed approach yields maximum response displacements which correlate very well with the persistency of real earthquakes for a bridge system with considerably complex (non-linear and non-smooth) behaviour.

References

Barenblatt G (1996) Scaling, self-similarity, and intermediate asymptotics. Cambridge University Press, Cambridge

DesRoches R, Muthukumar S (2002) Effect of pounding and restrainers on seismic response of multiple-frame bridges. J Struct Eng 128(7):860

Dicleli M (2008) Performance of seismic-isolated bridges with and without elastic-gap devices in near-fault zones. Earthq Eng Struct Dyn 37(6):935–954

Dimitrakopoulos EG (2010) Analysis of a frictional oblique impact observed in Skew bridges. Nonlinear Dyn 60:575–595

Dimitrakopoulos EG, Kappos AJ, Makris N (2009a) Dimensional analysis of yielding and pounding structures for records without distinct pulses. Soil Dyn Earthq Eng 29(7):1170–1180

Dimitrakopoulos EG, Makris N, Kappos AJ (2009b) Dimensional analysis of the earthquake-induced pounding between adjacent structures. Earthq Eng Struct Dyn 38(7):867–886

Dimitrakopoulos EG, Makris N, Kappos AJ (2010) Dimensional analysis of the earthquake response of a pounding oscillator. J Eng Mech (ASCE) 136(3):299–310

Jankowski R, Wilde K, Fujino Y (1998) Pounding of superstructure segments in isolated elevated bridge during earthquakes. Earthq Eng Struct Dyn 27(5):487–502

Leine RI, Van Campen DH, Glocker CH (2003) Nonlinear dynamics and modeling of various wooden toys with impact and friction. J Vib Control 9(1–2):25–78

Makris N, Chang S (2000) Effect of viscous, viscoplastic and friction damping on the response of seismic isolated structures. Earthq Eng Struct Dyn 29(1):85–107

Makris N, Black CJ (2004a) Dimensional analysis of rigid-plastic and elastoplastic structures under pulse-type excitations. J Eng Mech 130(9):1006

Makris N, Black CJ (2004b) Dimensional analysis of bilinear oscillators under pulse-type excitations. J Eng Mech 130(9):1019

Makris N, Psychogios T (2006) Dimensional response analysis of yielding structures with first-mode dominated response. Earthq Eng Struct Dyn 35(10):1203–1224

Malhotra PK (1998) Dynamics of seismic pounding at expansion joints of concrete bridges. J Eng Mech 124(7):794

Malhotra PK, Huang MJ, Shakal AF (1995) Seismic interaction at separation joints of an instrumented concrete bridge. Earthq Eng Struct Dyn 24(8):1055–1067

Rathje EM, Abrahamson NA, Bray JD (1998) Simplified frequency content estimates of earthquake ground motions. J Geotech Geoenviron Eng 124(2):150

Ruangrassamee A, Kawashima K (2001) Relative displacement response spectra with pounding effect. Earthq Eng Struct Dyn 30(10):1511–1538

Saadeghvaziri M, Yazdanimotlagh A (2008) Seismic behavior and capacity/demand analyses of three multi-span simply supported bridges. Eng Struct 30(1):54–66

Saadeghvaziri M, Yazdani-Motlagh AR, Rashidi S (2000) Effects of soil–structure interaction on longitudinal seismic response of MSSS bridges. Soil Dyn Earthq Eng 20(1–4):231–242

Sedov L (1992) Similarity and dimensional methods in mechanics. CRC Press, Boca Raton Fla

Vega J, del Rey I, Alarcon E (2009) Pounding force assessment in performance-based design of bridges. Earthq Eng Struct Dyn 38(13):1525–1544

Wen Y (1975) Approximate method for nonlinear random vibration 102(EM4):389–401

Wen Y (1976) Method for random vibration of hysteretic systems 102(EM2):249–263

Zanardo G, Hao H, Modena C (2002) Seismic response of multi-span simply supported bridges to a spatially varying earthquake ground motion. Earthq Eng Struct Dyn 31(6):1325–1345